DiVA
http://www.diva-portal.org

This is the published version of a paper published in *Geophysical Research Letters*.

Citation for the original published paper (version of record):

Zhu, M., Pastor–Galán, D., Smit, M A., Sanchir, D., Zhang, F. et al. (2024)
The Beginning of a Wilson Cycle in an Accretionary Orogen: The Mongol–Okhotsk Ocean Opened Assisted by a Devonian Mantle Plume
Geophysical Research Letters, 51(10)
https://doi.org/10.1029/2024gl109028

Access to the published version may require subscription.

N.B. When citing this work, cite the original published paper.

Permanent link to this version:
http://urn.kb.se/resolve?urn=urn:nbn:se:nrm:diva-5865

Check for updates

Geophysical Research Letters

RESEARCH LETTER
10.1029/2024GL109028

The Beginning of a Wilson Cycle in an Accretionary Orogen: The Mongol–Okhotsk Ocean Opened Assisted by a Devonian Mantle Plume

Mingshuai Zhu[1,2], Daniel Pastor–Galán[3,4], Matthijs A. Smit[5], Dorjgochoo Sanchir[1,2], Fuqin Zhang[1,2], Chenghao Liu[1,2], Ye Luo[1,2], and Laicheng Miao[1,2]

[1]Key Laboratory of Mineral Resources, Institute of Geology and Geophysics, Chinese Academy of Sciences, Beijing, China, [2]Innovation Academy for Earth Science, Chinese Academy of Sciences, Beijing, China, [3]Spanish National Research Council, Madrid, Spain, [4]Frontier Research Institute for Interdisciplinary Sciences, Tohoku University, Sendai, Japan, [5]Department of Earth, Ocean and Atmospheric Sciences, University of British Columbia, Vancouver, BC, Canada

Abstract The opening of oceans within accretionary orogens is important for understanding the Wilson cycle. The Mongol–Okhotsk Ocean (MOO) began opening within the early Paleozoic accretionary collage of the Central Asian Orogenic Belt (CAOB), representing a world-class example to constrain the geodynamic history of ocean opening in accretionary orogens, but the kinematics and mechanisms associated to this process are highly debated. We report on a newly-discovered bimodal volcanic suite and associated volcanic-sediments that comprise part of the Altay-Sayan Rift System, which indicate a widespread Early Devonian extensional event within the CAOB. This extension regime is attributed to a Devonian mantle plume, which is thought to have impinged upon and weakened the lithosphere of the Early Paleozoic collage, and drove the opening of the MOO. Opening of the MOO suggests continent breakup in accretionary orogens tends to focus along intervening weak orogenic lithosphere between the rigid microcontinents.

Plain Language Summary The opening of oceans within subduction related accretionary orogens is a process that is common within the geologic record. The tectonic mechanisms involved in this process, however, are not well understood. The Mongol–Okhotsk Ocean began opening within the Early Paleozoic accretionary collage of the Central Asian Orogenic Belt, providing an opportunity to constrain the geodynamic history of ocean opening in accretionary orogens, but the kinematics and mechanisms related to this process are highly debated. We report on newly-discovered bimodal volcanic suite (410–415 Ma) and associated volcanic-sedimentary rocks in Northwest Mongolia, which comprise part of the Altay-Sayan Rift System (also termed Altay-Sayan Large Igneous Province). This giant rift system represents a widespread Early Devonian extensional event associated with a mantle plume. The ascent of this mantle plume is thought to have impacted and weakened the lithosphere of northern Early Paleozoic collage, ultimately leading to the opening of the Mongol-Okhotsk Ocean between microcontinents that had earlier accreted to Siberia Craton. Our model suggests continent breakup in accretionary orogens tends to focus along weak orogenic lithosphere between the rigid microcontinents.

Key Points:

- The 415–410 Ma bimodal volcanic suite and associated volcanic-sediments document a widespread extension regime related to a mantle plume
- The Devonian mantle plume weakened structures within the accretionary orogen and led to the opening of the Mongol-Okhotsk Ocean
- Continent breakup in accretionary orogens tends to happen along weak orogenic lithosphere between rigid microcontinents

Supporting Information:

Supporting Information may be found in the online version of this article.

Correspondence to:

M. Zhu and L. Miao,
zhumingshuai@mail.iggcas.ac.cn;
miaolc@mail.iggcas.ac.cn

Citation:

Zhu, M., Pastor–Galán, D., Smit, M. A., Sanchir, D., Zhang, F., Liu, C., et al. (2024). The beginning of a Wilson cycle in an accretionary orogen: The Mongol–Okhotsk Ocean opened assisted by a Devonian mantle plume. *Geophysical Research Letters*, *51*, e2024GL109028. https://doi.org/10.1029/2024GL109028

Received 26 FEB 2024
Accepted 5 MAY 2024

Author Contributions:

Conceptualization: Mingshuai Zhu, Daniel Pastor–Galán, Matthijs A. Smit, Fuqin Zhang, Laicheng Miao
Data curation: Mingshuai Zhu, Daniel Pastor–Galán, Dorjgochoo Sanchir, Ye Luo
Formal analysis: Mingshuai Zhu, Chenghao Liu, Ye Luo
Investigation: Mingshuai Zhu, Daniel Pastor–Galán, Dorjgochoo Sanchir, Fuqin Zhang, Chenghao Liu, Ye Luo, Laicheng Miao
Methodology: Mingshuai Zhu, Dorjgochoo Sanchir, Chenghao Liu

© 2024. The Author(s).
This is an open access article under the terms of the Creative Commons Attribution License, which permits use, distribution and reproduction in any medium, provided the original work is properly cited.

1. Introduction

Precise constraints on continental breakup and consequent birth of new oceans play a key role in paleogeographic and tectonic models as they represent the initiation of the Wilson cycle (Brune et al., 2023; Wilson, 1966). Continental breakup has generally been attributed to either dynamic stresses imparted by uprising subcontinental mantle plumes (e.g., Cande & Stegman, 2011; Koptev et al., 2015), the tensional far-field stresses from slab rollback (e.g., Bercovici & Long, 2014; Dal Zilio et al., 2018), or the far-field effects of slab pull forces on the opposite margin of the same plate (e.g., following oceanic ridge subduction, Murphy et al., 2006; Wan et al., 2021). The mantle plume scenario is characterized by occurrence of large igneous provinces (LIPs), including flood basalts or silicic magmatic events (e.g., Bryan & Ernst, 2008; Torsvik et al., 2010). The slab rollback scenario is characterized by oceanward magmatic migration along the continental margin accompanied by back-arc extensions (Bercovici & Long, 2014; Nakakuki & Mura, 2013) that produced mafic magmas with geochemical variations between mid-ocean ridge basalt (MORB) and island-arc basalt (IAB) composition (e.g., Pearce & Stern, 2006). The far-field ridge subduction could give rise to a variety of rock assemblages, including MORB, A-type granites, adakites, Nb-enriched basalts and charnockites (e.g., Windley & Xiao, 2018). Thus, the

Software: Mingshuai Zhu, Dorjgochoo Sanchir
Supervision: Daniel Pastor–Galán, Matthijs A. Smit, Fuqin Zhang, Laicheng Miao
Validation: Mingshuai Zhu, Daniel Pastor–Galán
Visualization: Mingshuai Zhu, Daniel Pastor–Galán, Matthijs A. Smit, Fuqin Zhang, Chenghao Liu, Laicheng Miao
Writing – original draft: Mingshuai Zhu
Writing – review & editing: Mingshuai Zhu, Daniel Pastor–Galán, Matthijs A. Smit, Dorjgochoo Sanchir, Laicheng Miao

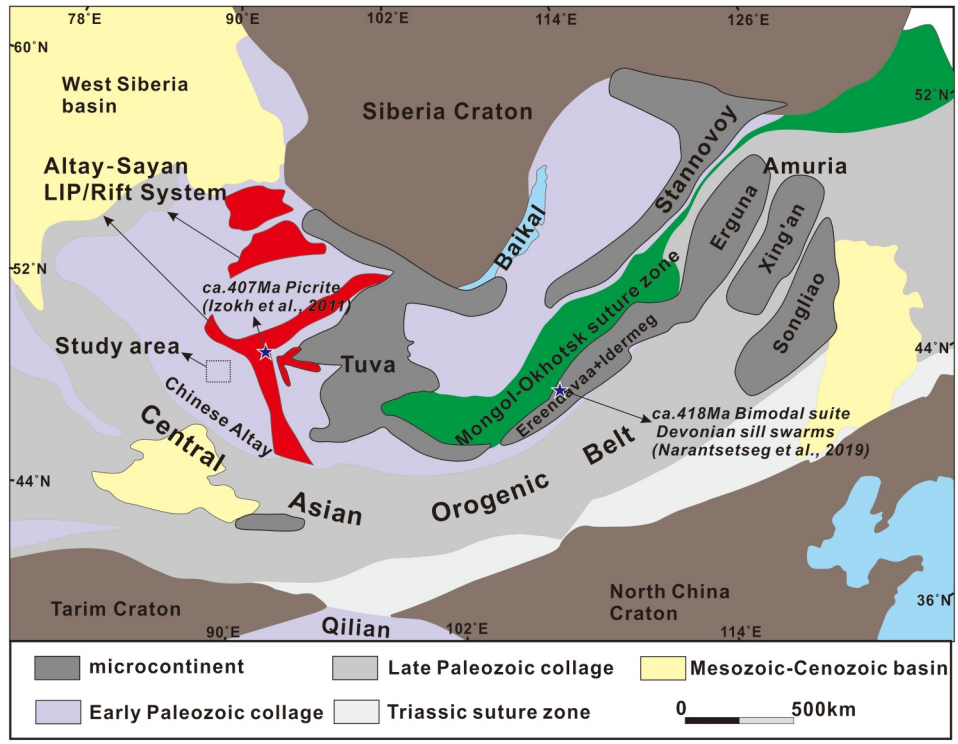

Figure 1. Tectonic map of Central Asia showing the positions of Altai-Sayan LIP/Rift System and Mongol-Okhotsk orogenic belt within the Central Asian Orogenic Belt (Modified from Zhou et al., 2018; Vorontsov et al., 2021).

magmatic record associated with the continent breakup can distinguish the dynamic driving forces of continent breakup and ocean opening.

A valuable field site where continental break-up can be studied for all its complexity and dynamics is the Central Asian Orogenic Belt (CAOB)—one of the largest accretionary collages in the world. The belt formed through multiple convergence and collisional events of various orogenic components from 1,000 to 250 Ma (e.g., Xiao et al., 2015). The peri-Siberian sector of the orogen mainly consists of microcontinents and Neoproterozoic-Cambrian subduction-accretionary complexes, which had been accreted to Siberia craton during Early Paleozoic related to the closure of the Pan-Rodinian Mirovoi Ocean (e.g., Buriánek et al., 2017; Wilhem et al., 2012; Zhu, Zhang, et al., 2023). The southern part of the CAOB predominantly comprises Mid to Late Paleozoic subduction-accretionary complex of the Paleo-Asian Ocean (e.g., Wilhem et al., 2012; Windley et al., 2007). The northern Early Paleozoic collage is crosscut by the young Mongol-Okhotsk orogenic belt, which preserves the evolution of the Mongol–Okhotsk Ocean (MOO) (Zorin, 1999; Figure 1). This Early Paleozoic orogenic domain is considered to be the site where the MOO opened during the Early–Middle Paleozoic (e.g., Domeier, 2018; Wilhem et al., 2012). These relationships provide the opportunity to investigate how accretionary orogens can be torn apart to form a new oceanic basin. The lack of precise constraints on kinematics, timing and mechanisms for the opening of the MOO has produced three contrasting models: (a) the MOO opened during Ediacaran-Cambrian times between the Siberian craton and the Tuva-Mongol massif (Sengör et al., 1993); (b) the MOO was a large embayment of the Paleo-Pacific, that opened in the Early Carboniferous-earliest Permian after the amalgamation of the Central Mongolian microcontinent and the Siberian Craton (e.g., Zorin, 1999); (c) the MOO opened by back-arc spreading during the latest Ordovician-Silurian within the Early Paleozoic collage of the CAOB (Bussien et al., 2011; Domeier, 2018). These models are speculative because the critical magmatic records of the initial MOO opening have not yet been found.

In this paper, we present new geochronological and geochemical data for Devonian bimodal magmatism and associated volcanic-sedimentary rocks in Northwest Mongolia. Integrated with the available records of the MOO, we propose a new tectono-magmatic scenario where the MOO opened in response to Devonian mantle plume

19448007, 2024, 10, Downloaded from https://agupubs.onlinelibrary.wiley.com/doi/10.1029/2024GL109028 by Naturhistoriska Riksmuseet, Wiley Online Library on [15/12/2024]. See the Terms and Conditions (https://onlinelibrary.wiley.com/terms-and-conditions) on Wiley Online Library for rules of use; OA articles are governed by the applicable Creative Commons License

19448007, 2024, 10, Downloaded from https://agupubs.onlinelibrary.wiley.com/doi/10.1029/2024GL109028 by Naturhistoriska Riksmuseet, Wiley Online Library on [15/12/2024]. See the Terms and Conditions (https://onlinelibrary.wiley.com/terms-and-conditions) on Wiley Online Library for rules of use; OA articles are governed by the applicable Creative Commons License

upwelling, which weakened the crust of the Early Paleozoic accretionary orogen and resulted in continent breakup along weak orogenic lithosphere between the rigid microcontinents previously accreted to Siberia.

2. Geological Setting and Analytical Methods

The Mongol-Okhotsk orogenic belt extends more than 3,000 km from central Mongolia to the Uda Gulf in the Okhotsk Sea (Figure 1; Zorin, 1999; Bussien et al., 2011). Concentric horseshoe-shaped microcontinental ribbons and magmatic-arc belts, and U-shaped aeromagnetic pattern suggest the Mongol-Okhotsk orogenic belt has an arcuate geometry and likely represents an orocline that developed during the closure of the MOO between Siberian Craton and the Amur Block (Xiao et al., 2015; Zorin, 1999). The MOO began subducting during the Pennsylvanian (Zhu, Pastor-Galán, et al., 2023) and was consumed by subduction on both of its margins, southward under the Amur Block and northward under the Siberian Craton (Donskaya et al., 2013). The final closure of the MOO is estimated to have occurred between the Early–Middle Jurassic and Early Cretaceous, leading to the collision of the Siberian Craton with the Amur Block (e.g., Van der Voo et al., 2015; Yi & Meert, 2020).

We report in this paper a newly discovered bimodal volcanic suite found about 30 km north of the Ulgey city, Mongolia, around the hinge of the curved Mongol-Okhotsk orogenic belt (Figure 1; Figure S1 in Supporting Information S1). The Ulgey bimodal suite with a thickness of up to 400 m consists of alternating units of basaltic andesite-rhyolite association (Figure 2a). The suite is intercalated with the Early Devonian Tunget formation, which consists of conglomerate, tuff sandstone, felsic tuff, rhyolite, sandstone and limestone (Filippova et al., 1990). The Late-Devonian Sagsai formation consists of sandstone, conglomerate, mudstone, basalt, rhyolite and carbonate rock (Filippova et al., 1990). The presumed Silurian Mukhar formation consists of mudstone, sandstone, siltstone, basalt, rhyolite, tuff with interbedded conglomerate (Figure 2b), and is underlain by Cambrian to Early Ordovician Mongol Altai formation composed of metamorphosed and isoclinally folded flysch-like sequences (Badarch et al., 2002; Figure S1 in Supporting Information S1).

To obtain the age of the Ulgey bimodal suite and provenance information of the Cambrian-Devonian sedimentary rocks, two rhyolites from the Ulgey bimodal suite of the Tunget formation, three sandstones from the Mongol Altai formation, one siltstone from the Mukhar formation, and three sandstone/siltstone from the Sagsai formation (detailed sample locations shown in Figure S1 in Supporting Information S1) were selected for U-Pb zircon dating by laser ablation inductively coupled plasma mass spectrometry (LA-ICP-MS). Whole-rock major and trace-element compositions, and Nd isotope compositions for the Ulgey bimodal magmatic suite and basalts from the Mukhar formation were determined by X-ray fluorescence (XRF), ICP-MS and multi-collector (MC) ICP-MS, respectively. The detailed analytical procedures can be found in Supporting Information S1.

3. Results

3.1. Zircon U-Pb Geochronology

The zircon U-Pb age results of 9 analyzed samples are given in Table S1 in Supporting Information S1 and Figures 2c and 2d. Zircons from two rhyolite samples 19MAT-169 and 19MAT-157 are euhedral to subhedral prisms that are 100–300 μm long. Most zircons show oscillatory zoning (Figure S2 in Supporting Information S1), a feature characteristic of igneous zircons. The measured U and Th concentrations vary from 54 to 3,283 ppm and from 28 to 6,078 ppm, respectively, with Th/U ratios between 0.41 and 1.20, also indicating an origin of igneous zircon (e.g., Rubatto, 2002). Fifteen analyses of sample 19MAT-169 yield a weighted mean $^{206}Pb/^{238}U$ age of 410 ± 4 Ma (MSWD = 0.89; Figure 2c), and 25 analyses of sample 19MAT-157 yield a weighted mean $^{206}Pb/^{238}U$ age of 415 ± 4 Ma (MSWD = 0.26; Figure 2c). Two analyses of sample 19MAT-169 yield older ages (ca. 2,312 Ma and 541 Ma), which are interpreted to record inheritance.

Most of the detrital zircon grains from the siltstone/sandstone samples in this study are euhedral to subhedral with clear oscillatory zoning (Figure S2 in Supporting Information S1). Samples 19MAT-33 (sandstone), 19MAT-193 (sandstone) and 19MAT-225 (sandstone) from the Mongol Altai formation yield mainly Cambrian to Early Ordovician and Neoproterozoic ages with minor Paleo-Mesoproterozoic ages, and they have a prominent ~512–510 Ma age peak (Figure 2d). Sample 19MAT-147 (siltstone) from the Mukhar formation mainly yields Cambrian to Early Ordovician, Early Devonian and Neoproterozoic ages with minor Silurian and Paleoproterozoic ages, and it has age peaks of ~408 and ~497 Ma (Figure 2d). Sample 19MAT-146 (siltstone), 19MAT-27 (sandstone) and 19MAT-09 (sandstone) from the Sagsai formation mainly yield Early-Middle Devonian and

10.1029/2024GL109028

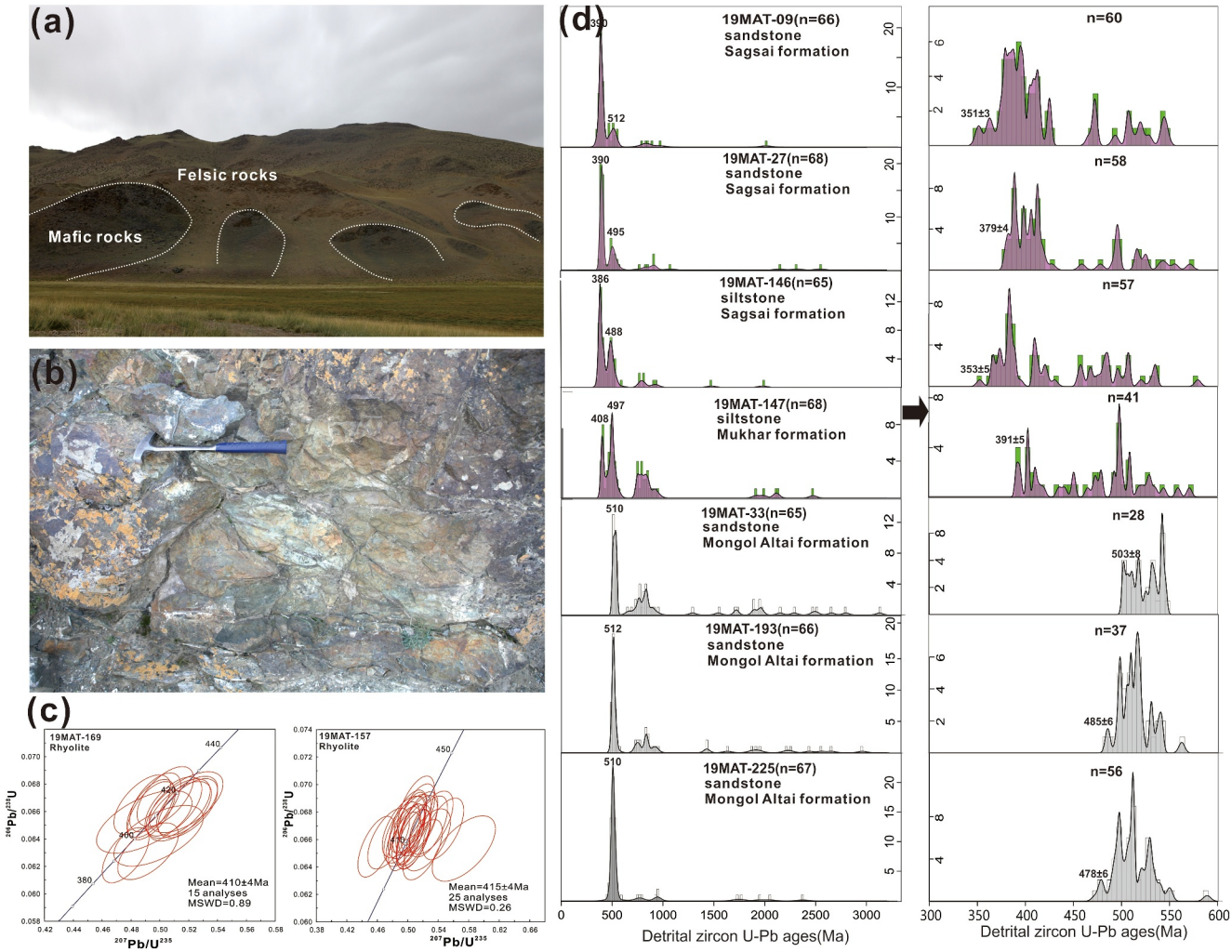

Figure 2. Field occurrences and zircon U-Pb results for the Ulgey bimodal volcanic suite and associated formations. (a) The Ulgey bimodal volcanic suite; (b) basalts from the Silurian Mukhar formation; (c) zircon U-Pb concordia plots of the two rhyolites from the Ulgey bimodal suite; (d) detrital zircon U-Pb ages for the Cambrian-Devonian sedimentary rocks.

Cambrian to Early Ordovician ages, with minor Late Devonian-Early Carboniferous, Neoproterozoic and Paleoproterozoic ages, and age peaks of ~386–390 Ma and ~488–512 Ma (Figure 2d).

3.2. Geochemistry

Whole-rock major- and trace-element data are given in Tables S2 and S3, and the Nd isotope results are presented in Table S4 in Supporting Information S1. The mafic rocks from the Ulgey bimodal volcanic suite have SiO_2 contents of 52.94–57.28 wt.%, and Al_2O_3, MgO, Na_2O, and TiO_2 contents of 13.17–14.47 wt.%, 2.70–5.63 wt.%, 3.79–5.25 wt.%, and 1.77–2.21 wt.%, respectively. They have moderate LREE/HREE ratios [$(La/Yb)_N$ of 2.1–5.6 and $(La/Sm)_N$ of 0.9–2.2] and either no anomaly or weak negative Eu anomalies (Eu/Eu* = 0.61–1.07) (Figure 3b). In the primitive mantle normalized spider diagram, they are enriched in LILE, LREEs and negative anomalies in Nb, Ta, Sr, and Ti (Figure 3a).

The felsic rocks from the Ulgey bimodal suite are characterized by high SiO_2 (72.3–77.3 wt.%) and K_2O (5.66–7.45 wt.%) contents with high K_2O/Na_2O ratios (9.95–40.98), but low MgO (0.47–0.72 wt.%) and CaO (0.07–0.85 wt.%) contents. The felsic samples show moderate LREE/HREE ratios [$(La/Yb)_N$ of 2.9–5.5 and $(La/Sm)_N$ of 2.0–2.8] and strong negative Eu anomalies (Eu/Eu* = 0.34–0.59) (Figure 3d). In the primitive mantle normalized spider diagram, the felsic samples have strong negative anomalies in Nb, Ta, Sr, and Ti (Figure 3c).

19448007, 2024, 10, Downloaded from https://agupubs.onlinelibrary.wiley.com/doi/10.1029/2024GL109028 by Naturhistoriska Riksmuseet, Wiley Online Library on [15/12/2024]. See the Terms and Conditions (https://onlinelibrary.wiley.com/terms-and-conditions) on Wiley Online Library for rules of use; OA articles are governed by the applicable Creative Commons License

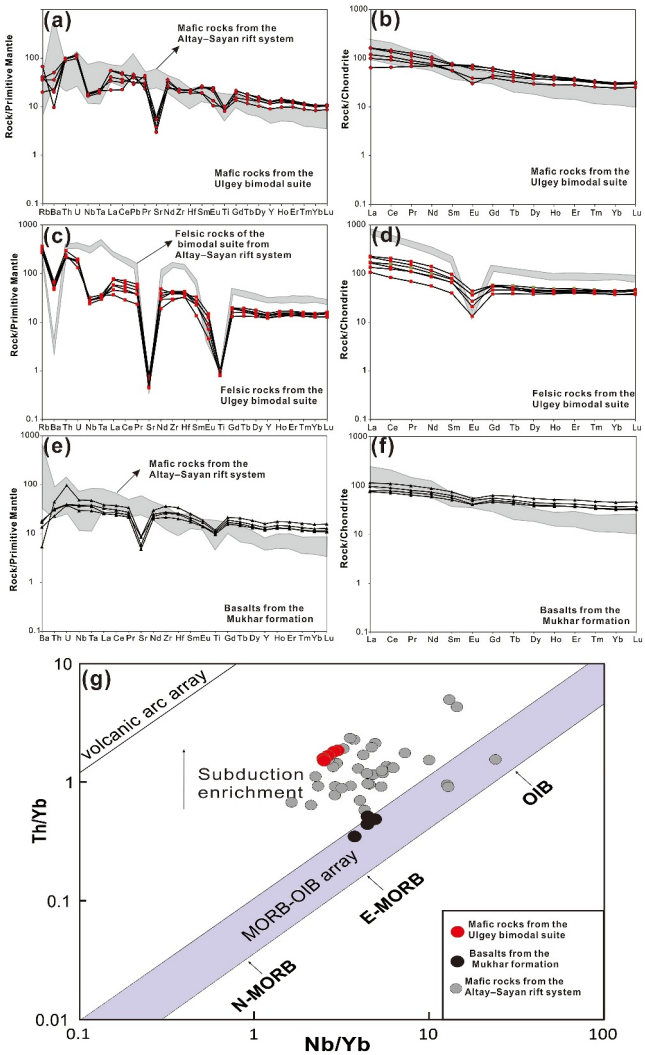

Figure 3. Geochemical plots of the Ulgey bimodal volcanic suite and the basalts from the Silurian Mukhar formation. (a, b) Primitive–mantle normalized diagrams and chondrite–normalized REE patterns for the mafic rocks from the Ulgey bimodal volcanic suite; (c, d) Primitive–mantle normalized diagrams and chondrite–normalized REE patterns for the felsic rocks from the Ulgey bimodal volcanic suite; (e, f) Primitive–mantle normalized diagrams and chondrite–normalized REE patterns for the basalts from the Silurian Mukhar formation; (g) Th/Yb–Nb/Yb diagram (J. A. Pearce, 2008) for the mafic rocks from the Ulgey bimodal suite, the Silurian Mukhar formation and the Altay-Sayan LIP/Rift System. Normalizing values are from Sun & McDonough (1989) for both chondrite and primitive mantle. The data of the Altay-Sayan LIP/Rift System are from Vorontsov et al. (2021) for comparison.

The basalt rocks from the Mukhar formation have SiO_2 of 47.46–48.82 wt%, MgO of 5.34–6.00 wt%, Al_2O_3 of 13.82–15.39 wt%, TiO_2 of 2.10–2.55 wt%. They have moderate LREE/HREE ratios [$(La/Yb)_N$ of 2.26–2.62 and $(La/Sm)_N$ of 1.39–1.54] and weak negative Eu anomalies ($Eu/Eu^* = 0.79–0.84$) (Figure 3f). In the primitive mantle normalized spider diagram, they show no Nb and Ta depletion, but show Sr and Ti depletion (Figure 3e).

Four mafic and four felsic volcanic samples from the Ulgey bimodal suite, and three basalt samples from the Mukhar formation were analyzed for Nd isotopes. The mafic rocks from the Ulgey bimodal suite have rather uniform radiogenic $\varepsilon_{Nd(t)}$ values ranging from +0.9 to +1.6, and the felsic samples have radiogenic $\varepsilon_{Nd(t)}$ values of +1.3–2.1. The basaltic samples from the Mukhar formation have significantly higher radiogenic $\varepsilon_{Nd(t)}$ values of +6.3 to +6.7.

4. Discussion

4.1. Significance of the Results

The rhyolites collected from the Ulgey bimodal suite in this study yielded a zircon age of 415–410 Ma, which we interpret as the crystallization age of the bimodal volcanic suite from the Early Devonian Tunget formation. The youngest detrital zircon ages we found in the Mongol Altai formation (ca. 503 and 478 Ma) mark a maximum depositional age which is consistent with its previous estimated Late Cambrian- Early Ordovician age. The youngest zircon ages (391 Ma) in the Mukhar Formation suggest an Early Devonian age rather than Silurian. The samples from the Sagsai Formation yielded significantly younger zircon ages (379–351 Ma), indicating the sedimentation lasted at least until the Late Devonian-Early Carboniferous. The Precambrian detritus in the samples was potentially derived from the basement of the Mongolian continental blocks and their overlying Tonian continental arc magmatism (e.g., Badarch et al., 2002; Jiang et al., 2017). The Cambrian-Early Ordovician age populations match the ages of the Ikh-Mongol Arc System (570–460 Ma; Janoušek et al., 2018). We interpret the Early Devonian detrital zircon signature of the Mukhar and Sagsai formations to be derived from erosion of the bimodal volcanic suites. According to these new results, a revised stratigraphic column for the Ulgey region is shown in Figure S3 in Supporting Information S1.

In principle, crustal contamination could have affected the compositions of mantle-derived magmas. However, the lack of correlation of Nb/La and Th/La, and of $\varepsilon_{Nd(t)}$ with SiO_2 rule out significant crustal contamination for the mafic rocks of the Ulgey bimodal suite (Figures S4a and S4b in Supporting Information S1). The mafic rocks have higher SiO_2 contents, but lower $Mg^{\#}$, Cr, and Ni contents than those of the primitive mantle-derived magma, suggesting variable amounts of fractional crystallization. The positive correlation of Cr and Ni contents against $Mg^{\#}$, and Ni versus Cr and V versus Cr diagrams indicate the likelihood of the fractional crystallization of olivine and clinopyroxene (Figures S5a–S5d in Supporting Information S1). The lack of correlation between the Dy/Yb ratios and SiO_2 contents, and between TiO_2 and MgO contents imply that amphibole and Fe-Ti oxide fractionation did not play a major role during the magmatic evolution (Figures S5e and S5f in Supporting Information S1). The mafic rocks from the Ulgey bimodal suite have low $(La/Yb)_N$ (2.1–5.6) and $(Tb/Yb)_N$ (1.04–1.35) ratios, and high HREE contents, indicating they were derived by partial melting of shallow spinel-bearing peridotites (Rooney, 2010). They are characterized by negative Nb, Ta, and Ti anomalies, are enriched in LILE, and plot above the MORB-OIB array (Figure 3g), suggesting their mantle source was modified by subduction-driven metasomatism (e.g., Clift et al., 2009; Gill, 1981; Pearce et al., 2021). In summary, the arc signatures and the positive $\varepsilon_{Nd(t)}$ for

19448007, 2024, 10, Downloaded from https://agupubs.onlinelibrary.wiley.com/doi/10.1029/2024GL109028 by Naturhistoriska Riksmuseet, Wiley Online Library on [15/12/2024]. See the Terms and Conditions (https://onlinelibrary.wiley.com/terms-and-conditions) on Wiley Online Library for rules of use; OA articles are governed by the applicable Creative Commons License

19448007, 2024, 10, Downloaded from https://agupubs.onlinelibrary.wiley.com/doi/10.1029/2024GL109028 by Naturhistoriska Riksmuseet, Wiley Online Library on [15/12/2024]. See the Terms and Conditions (https://onlinelibrary.wiley.com/terms-and-conditions) on Wiley Online Library for rules of use; OA articles are governed by the applicable Creative Commons License

mafic rocks can best be interpreted to be the result of varying degrees of partial melting of a depleted lithospheric mantle that was metasomatized by subduction-derived components.

For the bimodal suite, two main models have been proposed for genesis of evolved felsic magma: (a) partial melting of crustal rocks (anatexis) or young underplated basalts (e.g., Frost et al., 2001; Mahoney et al., 2008); and (b) extensive fractional crystallization from common mantle-derived mafic magmas, with or without crust assimilation (e.g., Peccerillo et al., 2003). In the former model, the mafic and felsic rocks show distinctly different geochemical features and Sr–Nd isotopic ratios (e.g., McCurry & Rodgers, 2009). In the latter model, the mafic and felsic rocks would exhibit similar geochemical signatures and Sr–Nd isotopic compositions, with mafic rocks dominating volumetrically compared with felsic rocks. The rhyolite samples from the Ulgey bimodal suite are characterized by high silica and alkali contents, strong negative Eu anomalies, and high concentrations in Ga, Zr, Nb, Ce and Y, which are typical of geochemical features of A-type granites (Figure S6 in Supporting Information S1; e.g. Whalen et al., 1987), indicating they likely formed from partial melting of an anhydrous source (Collins et al., 2021). The absence of intermediate compositions and the larger volumes of the felsic rocks than the mafic rocks suggest that the felsic rocks were not likely formed by fractional crystallization from the coeval mafic magma. The felsic rocks have positive $\varepsilon_{Nd(t)}$ values (1.3–2.1), which are indistinguishable from the mafic rocks of the Ulgey bimodal suite, indicating that they were probably derived from partial melting of the underplated mafic rocks of the lower crust.

The lack of a correlation between Nb/La and Th/La, and $\varepsilon_{Nd(t)}$ with SiO_2, and the low Th/Ce (0.05–0.06) and Th/Ta (1.6–1.9) indicate negligible crustal contamination during the evolution of the basalts from the Mukhar formation (Figures S4a and S4b in Supporting Information S1). Their LREE enrichment and lack of Nb-Ta anomaly is similar to E-MORB, but they have higher REE contents than the typical E-MORB (Sun & McDonough, 1989). An E-MORB mantle source is further supported by all these basaltic samples falling in the E-MORB field on the Th/Yb versus Nb/Yb diagram (Figure 3g). The $(La/Sm)_N$ versus $(Sm/Yb)_N$ and Sm/Yb versus Sm diagrams imply that these E-MORB-like basalts formed by low degree partial melting (~5%) of a mantle peridotite in the transitional spinel-garnet stability field (Figure S7 in Supporting Information S1). Thus, we interpret these E-MORB-like basalts with high positive $\varepsilon_{Nd(t)}$ to have formed from partial melting of a depleted mantle that was not metasomatized by subduction-related components (Figure 3g), which is distinct from the mantle source of the mafic rocks from the bimodal suite.

4.2. Tectonomagmatic Setting

Bimodal magmatic suites are characteristic extensional tectonic settings, including plume-related continental rifts, incipient back-arc basins, subduction zones and post–collisional extensional settings (e.g., Meade et al., 2014; Shinjo & Kato, 2000). The Ulgey bimodal suite formed nearby and at the same time as the Altay–Sayan Rift System (also termed the Altay-Sayan LIP) (ca. 410–390 Ma; Figure 1), which is dominated by mafic volcanism and phonolites, trachytes, and commendites, as well as a bimodal volcanic suite with associated sediments (e.g., Izokh et al., 2011; Vorontsov et al., 2021). Coeval with this Altay–Sayan LIP/Rift system, an Early Devonian extensional regime associated with asthenospheric upwelling in the Chinese Altai region developed, accompanied by (a) newly formed extensional basins that contain bimodal volcanic suites (e.g., Chai et al., 2009), (b) high-temperature/low-pressure metamorphic terranes with extension-related sub-horizontal foliations (e.g., Jiang et al., 2022), (c) MORB-like mafic rocks and coeval S-type granites (e.g., Cai et al., 2010), (d) widespread deep crustal anataxis that produced migmatite-granite complex (Wang et al., 2021), (e) juvenile mantle source addition evidenced by the abrupt increase of zircon $\varepsilon_{Hf(t)}$ from various tectonic units (P. F. Li et al., 2019). There are three tectonic models proposed to explain the extensional environment indicated by all of these geologic features: ridge subduction (e.g., Cai et al., 2011), southward subduction retreat of the Paleo-Asian ocean (e.g., P. F. Li et al., 2019; Soejono et al., 2018), and the effects of a mantle plume (Ernst et al., 2020; Kravchinsky, 2012; Kuzmin et al., 2010; Vorontsov et al., 2021). The ridge subduction model requires some form of flat subduction that should have resulted in a compressional environment and tectonic erosion of the overriding plate (e.g., Antonijevic et al., 2015), which contradicts the widespread extensional features found in the Devonian rocks, and is inconsistent with the apparent absence of geochemically distinctive adakitic rocks (high MgO, Cr, Co and Ni contents) and N-MORB derived magmas (Wang et al., 2020). Slab rollback could result in back-arc extensions (e.g., Bercovici & Long, 2014), but is unable to explain the triple-junction configuration and within plate OIB-like basalts in the Altay–Sayan LIP/Rift System (Figure 3g; Vorontsov et al., 2021). Some extensional areas are remote (more than 1,000 km) from the subduction zone during Early Devonian (Figure 1). In addition,

19448007, 2024, 10, Downloaded from https://agupubs.onlinelibrary.wiley.com/doi/10.1029/2024GL109028 by Naturhistoriska Riksmuseet, Wiley Online Library on [15/12/2024]. See the Terms and Conditions (https://onlinelibrary.wiley.com/terms-and-conditions) on Wiley Online Library for rules of use; OA articles are governed by the applicable Creative Commons License

extension-related metamorphism and magmatism both occur in a broad region in a narrow time interval (420–380 Ma, peaking at ca. 400 Ma) and show no age migration trend (Cai et al., 2011; Chai et al., 2009; P. F. Li et al., 2019; Vorontsov et al., 2021), which is inconsistent with the slab rollback model. The Altay–Sayan LIP/Rift System encompasses a total area of 0.35×10^6 km^2, and magmatism on different sites occurred nearly simultaneously (Ernst et al., 2020; Kuzmin et al., 2010). If our study area and Chinese Altay are included as part of this context, the lateral extent of the Early Devonian LIP would be larger than previously thought. The basaltic rocks in the Altay–Sayan LIP include both high-Ti and low-Ti varieties, similar to many LIPs such as for example, Siberian Traps and Karoo LIP of South Africa (Vorontsov et al., 2021). In addition, ca. 407 Ma picrodolerites, considered to be important evidence for a mantle plume, are recognized in the center of a triple junction from the Altay–Sayan LIP/Rift System (Izokh et al., 2011; Kravchinsky, 2012). The mafic rocks with subduction features were likely derived from plume-induced melting of the lithospheric mantle that was previously metasomatized during the Early Paleozoic accretion/subduction event (Vorontsov et al., 2021). Taken together, the magmatism from the Altay–Sayan LIP/Rift was likely to have originated from the activity of mantle plumes (Kravchinsky, 2012; Kuzmin et al., 2010; Vorontsov et al., 2021).

4.3. Inception of the Wilson Cycle in the Accretionary Orogen

Mantle plumes are usually involved in the first stage of the Wilson cycle: breakup of continents and opening of ocean (e.g., Storey, 1995). In Northwest Mongolia, the Ulgey bimodal suite (410–415 Ma) likely documents initial continent rifting of the Early Paleozoic collage in the CAOB. As rifting continued, the basalts from the Mukhar formation (younger than 391 Ma) with E-MORB geochemical affinity likely result from partial melting of the upwelling asthenosphere influenced by the Early Devonian mantle plume. Thus, we suggest the basalts from the Mukhar Formation represent initial oceanic crust formation during early seafloor spreading, similar to the scenario of the young South China Sea where extensive E-MORB occurs along the seafloor (Larsen et al., 2018; Liao et al., 2022). In the Ereendavaa terrane along southern margin of the MOO, coeval bimodal volcanic rocks and alkaline riebeckite granites (418-409 Ma) document an Early Devonian extensional environment (Narantsetseg et al., 2019; Orolmaa et al., 2015). An extensional environment is also supported by the widespread occurrence of the Devonian diabase and gabbro-diabase sill swarms within the Early Devonian shallow marine molasse formations in this region (Narantsetseg et al., 2019), which is usually suggested to document continental lithospheric extension, continental rifting and breakup events (e.g., Bryan & Ernst, 2008). These records of extension are coeval with the Devonian Altay–Sayan LIP, suggesting the ascent of an Early Devonian mantle plume may have triggered the opening of the MOO. The age of the earliest rift-related sedimentation could provide constraints on the timing of continental breakup and the initiation of seafloor spreading. In the Ereendavaa terrane, the Neoproterozoic formations are unconformably overlain by Silurian clastic strata and Devonian volcanic and volcaniclastic rocks, and minor limestone (Badarch et al., 2002). Zircon U–Pb dating results indicate the Silurian-Devonian formation formed during latest Silurian- Early Devonian, probably related to the opening of the MOO (Miao et al., 2017). To the northeast, in the Jiamusi region of the Amuria block, the Middle Devonian Heitai Formation overlying the Precambrian basement consists of clastic rocks and carbonates, and is proposed to document the passive continental margin of the MOO at ca. 380 Ma (G. Y. Li et al., 2019). These records indicate that the MOO initially opened during Early Devonian and divided the Early Paleozoic collage of terranes previously assembled against the southeast margin of the Siberian Craton (Figure 4a). Paleomagnetic studies indicate that the Amuria blocks were located around Siberia during the Silurian, but differ by 30° in paleolatitude during the Devonian (Bretshtein & Klimova, 2007; Kravchinsky et al., 2002; Torsvik et al., 2012), indicating that the MOO between these terranes progressively widened by that time. Thus, we propose a new tectono-magmatic model in which the rising Devonian hot plume impinged upon the lithosphere of northern Early Paleozoic collage and further weakened and thinned the lithosphere to ultimately trigger the opening of the MOO. In addition, the MOO initiated between the microcontinents that accreted to Siberia Craton (Figure 1), likely because the microcontinental blocks with cratonic lithosphere represent rigid blocks within accretionary orogens (Zhou et al., 2018). The intervening weak orogenic lithosphere between the microcontinents guides the continent breakup and consequent ocean birth with the assistance of plume-induced lithospheric weakening.

5. Conclusions

The 415–410 Ma bimodal volcanic suite and associated volcanic-sedimentary rocks in northwest Mongolia comprise part of the Altay-Sayan LIP/Rift System, and represent a widespread Early Devonian extensional event

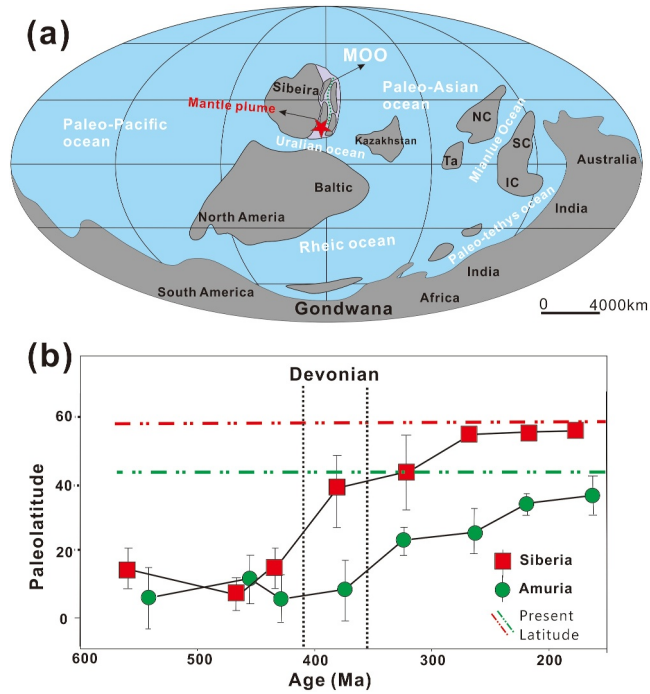

Figure 4. Early Devonian (410–415 Ma) global plate tectonic map (from Golonka et al., 2023) and paleolatitudes of the Amur Block and Siberia Craton during 600–150 Ma (from Bretshtein & Klimova, 2007; Liu et al., 2021).

within the northern Early Paleozoic collage of the CAOB. This Devonian extension regime is attributed to a mantle plume, which is thought to have impacted and weakened the lithosphere of northern Early Paleozoic collage ultimately leading to the opening of the MOO. Our model of MOO opening implies that the continent breakup in accretionary orogens tends to take place along intervening weak orogenic lithosphere between the rigid microcontinents.

Data Availability Statement

The Supporting Information S1 includes data collection techniques, supporting figures and captions for the supporting data sets (Tables S1–S4 in Supporting Information S1). All of the data sets were collected by the authors and are available in the Zenodo data repository (Zhu, 2024).

Acknowledgments
The authors thank the Editor Fabio A. Capitanio and three reviewers for their comments which helped improve the manuscript. This work was financially supported by Strategic Priority Research Program of Chinese Academy of Sciences (Grant XDB 41000000) and the National Natural Science Foundation of China (Grant 42272262).

References

Antonijevic, S. K., Wagner, L. S., Kumar, A., Beck, S. L., Long, M. D., Zandt, G., et al. (2015). The role of ridges in the formation and longevity of flat slabs. *Nature*, *524*(7564), 212–215. https://doi.org/10.1038/nature14648

Badarch, G., Cunningham, W. D., & Windley, B. F. (2002). A new terrane subdivision for Mongolia: Implications for the Phanerozoic crustal growth of Central Asia. *Journal of Asian Earth Sciences*, *21*(1), 87–104.

Bercovici, D., & Long, M. D. (2014). Slab rollback instability and supercontinent dispersal. *Geophysical Research Letters*, *41*(19), 6659–6666. https://doi.org/10.1002/2014gl061251

Bretshtein, Y. S., & Klimova, A. V. (2007). Paleomagnetic study of late Proterozoic and early Cambrian rocks in terranes of the Amur plate. *Izvestiya - Physics of the Solid Earth*, *43*(10), 890–903. https://doi.org/10.1134/s1069351307100114

Brune, S., Kolawole, F., Olive, J. A., Stamps, D. S., Buck, W. R., Buiter, S. J. H., et al. (2023). Geodynamics of continental rift initiation and evolution. *Nature Reviews Earth & Environment*, *4*(4), 235–253. https://doi.org/10.1038/s43017-023-00391-3

Bryan, S. E., & Ernst, R. E. (2008). Revised definition of large igneous provinces (LIPs). *Earth-Science Reviews*, *86*(1–4), 175–202. https://doi.org/10.1016/j.earscirev.2007.08.008

Buriánek, D., Schulmann, K., Hrdličková, K., Hanžl, P., Janoušek, V., Gerdes, A., & Lexa, O. (2017). Geochemical and geochronological constraints on distinct Early-Neoproterozoic and Cambrian accretionary events along southern margin of the Baydrag Continent in western Mongolia. *Gondwana Research*, *47*, 200–227. https://doi.org/10.1016/j.gr.2016.09.008

Bussien, D., Gombojav, N., Winkler, W., & von Quadt, A. (2011). The Mongol-Okhotsk Belt in Mongolia – An appraisal of the geodynamic development by the study of sandstone provenance and detrital zircons. *Tectonophysics*, *510*(1–2), 132–150. https://doi.org/10.1016/j.tecto.2011.06.024

Cai, K. D., Sun, M., Yuan, C., Zhao, G. C., Xiao, W. J., Long, X. P., & Wu, F. (2010). Geochronological and geochemical study of mafic dykes from the northwest Chinese Altai: Implications for petrogenesis and tectonic evolution. *Gondwana Research*, *18*(4), 638–652. https://doi.org/10.1016/j.gr.2010.02.010

19448007, 2024, 10, Downloaded from https://agupubs.onlinelibrary.wiley.com/doi/10.1029/2024GL109028 by Naturhistoriska Riksmuseet, Wiley Online Library on [15/12/2024]. See the Terms and Conditions (https://onlinelibrary.wiley.com/terms-and-conditions) on Wiley Online Library for rules of use; OA articles are governed by the applicable Creative Commons License

Cai, K. D., Sun, M., Yuan, C., Zhao, G. C., Xiao, W. J., Long, X. P., & Wu, F. (2011). Geochronology, petrogenesis and tectonic significance of peraluminous granites from the Chinese Altai, NW China. *Lithos*, *127*(1–2), 261–281. https://doi.org/10.1016/j.lithos.2011.09.001

Cande, S. C., & Stegman, D. R. (2011). Indian and African plate motions driven by the push force of the Reunion plume head. *Nature*, *475*(7354), 47–52. https://doi.org/10.1038/nature10174

Chai, F. M., Mao, J. W., Dong, L. H., Yang, F. Q., Liu, F., Geng, X. X., & Zhang, Z. (2009). Geochronology of metarhyolites from the Kangbutiebao formation in the Kelang basin, Altay Mountains, Xinjiang: Implications for the tectonic evolution and metallogeny. *Gondwana Research*, *16*(2), 189–200. https://doi.org/10.1016/j.gr.2009.03.002

Clift, P. D., Vannucchi, P., & Morgan, J. P. (2009). Crustal redistribution, crust-mantle recycling and Phanerozoic evolution of the continental crust. *Earth-Science Reviews*, *97*(1–4), 80–104. https://doi.org/10.1016/j.earscirev.2009.10.003

Collins, W. J., Murphy, J. B., Blereau, E., & Huang, H.-Q. (2021). Water availability controls crustal melting temperatures. *Lithos*, *402–403*, 106351. https://doi.org/10.1016/j.lithos.2021.106351

Dal Zilio, L., Faccenda, M., & Capitanio, F. (2018). The role of deep subduction in supercontinent breakup. *Tectonophysics*, *746*, 312–324. https://doi.org/10.1016/j.tecto.2017.03.006

Domeier, M. (2018). Early Paleozoic tectonics of Asia: Towards a full-plate model. *Geoscience Frontiers*, *9*(3), 789–862. https://doi.org/10.1016/j.gsf.2017.11.012

Donskaya, T. V., Gladkochub, D. P., Mazukabzov, A. M., & Ivanov, A. V. (2013). Late Paleozoic-Mesozoic subduction-related magmatism at the southern margin of the Siberian continent and the 150 million-year history of the Mongol-Okhotsk Ocean. *Journal of Asian Earth Sciences*, *62*, 79–97. https://doi.org/10.1016/j.jseaes.2012.07.023

Ernst, R. E., Rodygin, S. A., & Grinev, O. M. (2020). Age correlation of large igneous provinces with Devonian biotic crises. *Global and Planetary Change*, *185*, 103097. https://doi.org/10.1016/j.gloplacha.2019.103097

Filippova, I. V., Suetenko, O. D., & Levintov, M. E. (1990). *Explanation text to geological map of Western Mongolia, scale 1: 500,000. The volume 1, Stratigraphy*. Academia Nauka USSR.

Frost, C. D., Bell, J. M., Frost, B. R., & Chamberlain, K. R. (2001). Crustal growth by magmatic underplating: Isotopic evidence from the northern Sherman batholith. *Geology*, *29*(6), 515–518. https://doi.org/10.1130/0091-7613(2001)029<0515:cgbmui>2.0.co;2

Gill, J. B. (1981). *Orogenic andesites and plate tectonics* (p. 390). Springer-Verlag.

Golonka, J., Porebski, S. J., & Waskowska, A. (2023). Silurian paleogeography in the framework of global plate tectonics. *Palaeogeography, Palaeoclimatology, Palaeoecology*, *622*, 111597. https://doi.org/10.1016/j.palaeo.2023.111597

Izokh, A. E., Vishnevskii, A. V., Polyakov, G. V., & Shelepaev, R. A. (2011). Age of picrite and picrodolerite magmatism in western Mongolia. *Russian Geology and Geophysics*, *52*(1), 7–23. https://doi.org/10.1016/j.rgg.2010.12.002

Janoušek, V., Jiang, Y. D., Buriánek, D., Schulmann, K., Hanžl, P., Soejono, I., et al. (2018). Cambrian-Ordovician magmatism of the Ikh-Mongol Arc System exemplified by the Khantaishir magmatic complex (lake zone, south-central Mongolia). *Gondwana Research*, *54*, 122–149. https://doi.org/10.1016/j.gr.2017.10.003

Jiang, Y. D., Schulmann, K., Kröner, A., Sun, M., Lexa, O., Janoušek, V., et al. (2017). Neoproterozoic–early Paleozoic peri-Pacific accretionary evolution of the Mongolian collage system: Insights from geochemical and U–Pb zircon data from the Ordovician sedimentary wedge in the Mongolian Altai. *Tectonics*, *36*(11), 2305–2331. https://doi.org/10.1002/2017tc004533

Jiang, Y. D., Stípská, P., Schulmann, K., Aguilar, C., Wang, S., Anczkiewicz, R., et al. (2022). Barrovian and Buchan metamorphic series in the Chinese Altai: P-T-t-D evolution and tectonic implications. *Journal of Metamorphic Geology*, *40*(4), 823–857. https://doi.org/10.1111/jmg.12647

Koptev, A., Calais, E., Burov, E., Leroy, S., & Gerya, T. (2015). Dual continental rift systems generated by plume-lithosphere interaction. *Nature Geoscience*, *8*(5), 388–392. https://doi.org/10.1038/ngeo2401

Kravchinsky, V. A. (2012). Paleozoic large igneous provinces of Northern Eurasia: Correlation with mass extinction events. *Global and Planetary Change*, *86–87*, 31–36. https://doi.org/10.1016/j.gloplacha.2012.01.007

Kravchinsky, V. A., Sorokin, A. A., & Courtillot, V. (2002). Paleomagnetism of Paleozoic and Mesozoic sediments of southern margin of Mongol-Okhotsk Ocean, Far East of Russia. *Journal of Geophysical Research*, *107*(B10), 2253. https://doi.org/10.1029/2001jb000672

Kuzmin, M. I., Yarmolyuk, V. V., & Kravchinsky, V. A. (2010). Phanerozoic hot spot traces and paleogeographic reconstructions of the Siberian continent based on interaction with the African large low shear velocity province. *Earth-Science Reviews*, *102*(1–2), 29–59. https://doi.org/10.1016/j.earscirev.2010.06.004

Larsen, H. C., Mohn, G., Nirrengarten, M., Sun, Z., Stock, J., Jian, Z., et al. (2018). Rapid transition from continental breakup to igneous oceanic crust in the South China Sea. *Nature Geoscience*, *11*(10), 782–789. https://doi.org/10.1038/s41561-018-0198-1

Li, G. Y., Zhou, J. B., Wilde, S. A., & Li, L. (2019). The transition from a passive to an active continental margin in the Jiamusi Block: Constraints from Late Paleozoic sedimentary rocks. *Journal of Geodynamics*, *129*, 131–148. https://doi.org/10.1016/j.jog.2018.01.010

Li, P. F., Sun, M., Shu, C. T., Yuan, C., Jiang, Y. D., Zhang, L., & Cai, K. (2019). Evolution of the Central Asian orogenic belt along the Siberian margin from Neoproterozoic-early Paleozoic accretion to Devonian trench retreat and a comparison with Phanerozoic eastern Australia. *Earth-Science Reviews*, *198*, 102951. https://doi.org/10.1016/j.earscirev.2019.102951

Liao, R., Zhu, H., Li, C., & Sun, W. (2022). Geochemistry of mantle source during the initial expansion and its implications for the opening of the South China Sea. *Marine Geology*, *447*, 106798. https://doi.org/10.1016/j.margeo.2022.106798

Liu, Y. J., Li, W. M., Ma, Y. F., Feng, Z. Q., Guan, Q. B., Li, S. Z., et al. (2021). An orocline in the eastern Central Asian orogenic belt. *Earth-Science Reviews*, *221*, 103808. https://doi.org/10.1016/j.earscirev.2021.103808

Mahoney, J. J., Saunders, A. D., Storey, M., & Randriamanantenasoa, A. (2008). Geochemistry of the Volcan de l'Androy basalt-rhyolite complex, Madagascar cretaceous igneous province. *Journal of Petrology*, *49*(6), 1069–1096. https://doi.org/10.1093/petrology/egn018

McCurry, M., & Rodgers, D. W. (2009). Mass transfer along the Yellowstone hotspot track I: Petrologic constraints on the volume of mantle-derived magma. *Journal of Volcanology and Geothermal Research*, *188*(1–3), 86–98. https://doi.org/10.1016/j.jvolgeores.2009.04.001

Meade, F. C., Troll, V. R., Ellam, R. M., Freda, C., Font, L., Donaldson, C. H., & Klonowska, I. (2014). Bimodal magmatism produced by progressively inhibited crustal assimilation. *Nature Communications*, *5*(1), 4199. https://doi.org/10.1038/ncomms5199

Miao, L. C., Zhang, F. C., Baatar, M., Zhu, M. S., & Anaad, C. (2017). SHRIMP zircon U-Pb ages and tectonic implications of igneous events in the Ereendavaa metamorphic terrane in NE Mongolia. *Journal of Asian Earth Sciences*, *144*, 243–260. https://doi.org/10.1016/j.jseaes.2017.03.005

Murphy, J. B., Gutierrez-Alonso, G., Nance, R. D., Fernandez-Suarez, J., Keppie, J. D., Quesada, C., et al. (2006). Origin of the Rheic Ocean: Rifting along a Neoproterozoic suture? *Geology*, *34*(5), 325–328. https://doi.org/10.1130/g22068.1

Nakakuki, T., & Mura, E. (2013). Dynamics of slab rollback and induced back-arc basin formation. *Earth and Planetary Science Letters*, *361*, 287–297. https://doi.org/10.1016/j.epsl.2012.10.031

19448007, 2024, 10, Downloaded from https://agupubs.onlinelibrary.wiley.com/doi/10.1029/2024GL109028 by Naturhistoriska Riksmuseet, Wiley Online Library on [15/12/2024]. See the Terms and Conditions (https://onlinelibrary.wiley.com/terms-and-conditions) on Wiley Online Library for rules of use; OA articles are governed by the applicable Creative Commons License

Narantsetseg, T., Orolmaa, D., Yuan, C., Wang, T., Guo, L., Tong, Y., et al. (2019). Early-Middle Paleozoic volcanic rocks from the Ereendavaa terrane (Tsarigiin gol area, NE Mongolia) with implications for tectonic evolution of the Kherlen massif. *Journal of Asian Earth Sciences*, *175*, 138–157. https://doi.org/10.1016/j.jseaes.2018.12.008

Orolmaa, D., Turbold, S., & Odgerel, D. (2015). Lower Paleozoic granitoids of Undurkhaan district: Geochronology and geochemistry. *Explorer*, *53*, 54–68.

Pearce, J., Ernst, R., Peate, D., & Rogers, C. (2021). LIP printing: Use of immobile element proxies to characterize Large Igneous Provinces in the geologic record. *Lithos*, *392–393*, 106068. https://doi.org/10.1016/j.lithos.2021.106068

Pearce, J. A. (2008). Geochemical fingerprinting of oceanic basalts with applications to ophiolite classification and the search for Archean oceanic crust. *Lithos*, *100*(1–4), 14–48. https://doi.org/10.1016/j.lithos.2007.06.016

Pearce, J. A., & Stern, R. J. (2006). Origin of back-arc basin magmas: Trace element and isotope perspectives. In D. M. Christie, C. R. Fisher, S. M. Lee, & S. Givens (Eds.), *Geophysical monograph book series* (pp. 63–86).

Peccerillo, A., Barberio, M. R., Yirgu, G., Ayalew, D., Barbieri, M., & Wu, T. W. (2003). Relationships between mafic and peralkaline silicic magmatism in continental rift settings: A petrological, geochemical and isotopic study of the Gedemsa volcano, central Ethiopian rift. *Journal of Petrology*, *44*(11), 2003–2032. https://doi.org/10.1093/petrology/egg068

Rooney, T. O. (2010). Geochemical evidence of lithospheric thinning in the southern Main Ethiopian Rift. *Lithos*, *117*(1–4), 33–48. https://doi.org/10.1016/j.lithos.2010.02.002

Rubatto, D. (2002). Zircon trace element geochemistry: Partitioning with garnet and the link between U-Pb ages and metamorphism. *Chemical Geology*, *184*(1–2), 123–138. https://doi.org/10.1016/s0009-2541(01)00355-2

Sengor, A. M. C., Natalin, B. A., & Burtman, V. S. (1993). Evolution of the Altaid tectonic collage and Paleozoic crustal growth in Eurasia. *Nature*, *364*(6435), 299–307. https://doi.org/10.1038/364299a0

Shinjo, R., & Kato, Y. (2000). Geochemical constraints on the origin of bimodal magmatism at the Okinawa Trough, an incipient back-arc basin. *Lithos*, *54*(3–4), 117–137. https://doi.org/10.1016/s0024-4937(00)00034-7

Soejono, I., Cáp, P., Míková, J., Janousek, V., Buriánek, D., & Schulmann, K. (2018). Early Palaeozoic sedimentary record and provenance of flysch sequences in the Hovd Zone (western Mongolia): Implications for the geodynamic evolution of the Altai accretionary wedge system. *Gondwana Research*, *64*, 163–183. https://doi.org/10.1016/j.gr.2018.07.005

Storey, B. C. (1995). The role of mantle plumes in continental break-up: Case histories from Gondwanaland. *Nature*, *377*(6547), 301–308. https://doi.org/10.1038/377301a0

Sun, S. S., & McDonough, W. F. (1989). Chemical and isotopic systematics of oceanic basalts: Implications for mantle composition and processes. In A. D. Saunders, & M. J. Norry, (Eds.), *Magmatism in the ocean basins* (Vol. 42(1), pp. 313–345). *Geological Society, London, Special Publications*. https://doi.org/10.1144/gsl.sp.1989.042.01.19

Torsvik, T. H., Burke, K., Steinberger, B., Webb, S. J., & Ashwal, L. D. (2010). Diamonds sampled by plumes from the core-mantle boundary. *Nature*, *466*(7304), 352–355. https://doi.org/10.1038/nature09216

Torsvik, T. H., Van der Voo, R., Preeden, U., Mac Niocaill, C., Steinberger, B., Doubrovine, P. V., et al. (2012). Phanerozoic polar wander, palaeogeography and dynamics. *Earth-Science Reviews*, *114*(3–4), 325–368. https://doi.org/10.1016/j.earscirev.2012.06.007

Van der Voo, R., van Hinsbergen, D. J., Domeier, M., Spakman, W., & Torsvik, T. H. (2015). Latest Jurassic-earliest Cretaceous closure of the Mongol-Okhotsk Ocean: A paleomagnetic and seismological-tomographic analysis. *Geological Society of America Special Paper*, *513*, 589–606.

Vorontsov, A., Yarmolyuk, V., Dril, S., Ernst, R., Perfilova, O., Grinev, O., & Komaritsyna, T. (2021). Magmatism of the Devonian Altai-Sayan Rift System: Geological and geochemical evidence for diverse plume-lithosphere interactions. *Gondwana Research*, *89*, 193–219. https://doi.org/10.1016/j.gr.2020.09.007

Wan, B., Chu, Y., Chen, L., Liang, X. F., Zhang, Z. Y., Ao, S. J., & Talebian, M. (2021). Paleo-Tethys subduction induced slab-drag opening the Neo-Tethys: Evidence from an Iranian segment of Gondwana. *Earth-Science Reviews*, *221*, 103788. https://doi.org/10.1016/j.earscirev.2021.103788

Wang, J., Su, Y. P., Zheng, J. P., Belousova, E. A., Chen, M., Dai, H. K., & Zhou, L. (2020). Slab roll-back triggered back-arc extension south of the Paleo-Asian Ocean: Insights from Devonian MORB-like diabase dykes from the Chinese Altai. *Lithos*, *376*, 105790. https://doi.org/10.1016/j.lithos.2020.105790

Wang, S., Jiang, Y. D., Weinberg, R., Schulmann, K., Zhang, J., Li, P. F., et al. (2021). Flow of Devonian anatectic crust in the accretionary Altai Orogenic Belt, central Asia: Insights into horizontal and vertical magma transfer. *Geological Society of America Bulletin*, *133*(11–12), 2501–2523. https://doi.org/10.1130/b35645.1

Whalen, J. B., Currie, K. L., & Chappell, B. W. (1987). A-Type Granites - Geochemical characteristics, discrimination and petrogenesis. *Contributions to Mineralogy and Petrology*, *95*(4), 407–419. https://doi.org/10.1007/bf00402202

Wilhem, C., Windley, B. F., & Stampfli, G. M. (2012). The Altaids of Central Asia: A tectonic and evolutionary innovative review. *Earth-Science Reviews*, *113*(3–4), 303–341. https://doi.org/10.1016/j.earscirev.2012.04.001

Wilson, J. T. (1966). Did the Atlantic close and then re-open? *Nature*, *211*(5050), 676–681. https://doi.org/10.1038/211676a0

Windley, B. F., Alexeiev, D., Xiao, W. J., Kröner, A., & Badarch, G. (2007). Tectonic models for accretion of the Central Asian orogenic belt. *Journal of the Geological Society*, *164*(1), 31–47. https://doi.org/10.1144/0016-76492006-022

Windley, B. F., & Xiao, W. J. (2018). Ridge subduction and slab windows in the Central Asian Orogenic Belt: Tectonic implications for the evolution of an accretionary orogen. *Gondwana Research*, *61*, 73–87. https://doi.org/10.1016/j.gr.2018.05.003

Xiao, W. J., Windley, B. F., Sun, S., Li, J. L., Huang, B. C., Han, C. M., et al. (2015). A tale of amalgamation of three Permo-Triassic collage systems in Central Asia: Oroclines, sutures, and terminal accretion. *Annual Review of Earth and Planetary Sciences*, *43*(1), 477–507. https://doi.org/10.1146/annurev-earth-060614-105254

Yi, Z. Y., & Meert, J. G. (2020). A closure of the Mongol-Okhotsk Ocean by the middle Jurassic: Reconciliation of paleomagnetic and geological evidence. *Geophysical Research Letters*, *47*(15), e2020GL088235. https://doi.org/10.1029/2020gl088235

Zhou, J. B., Wilde, S. A., Zhao, G. C., & Han, J. (2018). Nature and assembly of microcontinental blocks within the Paleo-Asian Ocean. *Earth-Science Reviews*, *186*, 76–93. https://doi.org/10.1016/j.earscirev.2017.01.012

Zhu, M. S. (2024). The beginning of a Wilson cycle in an accretionary orogen [Dataset]. *Zenodo*. https://doi.org/10.5281/zenodo.11090227

Zhu, M. S., Pastor-Galán, D., Miao, L. C., Zhang, F. Q., Ganbat, A., Li, S., et al. (2023). Evidence for early Pennsylvanian subduction initiation in the Mongol-Okhotsk Ocean from the Adaatsag ophiolite (Mongolia). *Lithos*, 436–443.

Zhu, M. S., Zhang, F. Q., Smit, M. A., Pastor-Galan, D., Guilmette, C., Miao, L. C., et al. (2023). Discovery of a >1,000 km Cambrian eclogite-bearing high-pressure metamorphic belt in the Central Asian orogenic belt: Implications for the final closure of the Pan-Rodinian Ocean. *Journal of Geophysical Research-Solid Earth*, *128*(1), e2022JB025388. https://doi.org/10.1029/2022jb025388

19448007, 2024, 10, Downloaded from https://agupubs.onlinelibrary.wiley.com/doi/10.1029/2024GL109028 by Naturhistoriska Riksmuseet, Wiley Online Library on [15/12/2024]. See the Terms and Conditions (https://onlinelibrary.wiley.com/terms-and-conditions) on Wiley Online Library for rules of use; OA articles are governed by the applicable Creative Commons License

Zorin, Y. A. (1999). Geodynamics of the western part of the Mongolia-Okhotsk collisional belt, Trans-Baikal region (Russia) and Mongolia. *Tectonophysics*, *306*(1), 33–56. https://doi.org/10.1016/s0040-1951(99)00042-6

References From the Supporting Information

Aldanmaz, E., Köprübaşı, N., Gürer, Ö. F., Kaymakçi, N., & Gourgaud, A. (2006). Geochemical constraints on the Cenozoic, OIB-type alkaline volcanic rocks of NW Turkey: Implications for mantle sources and melting processes. *Lithos*, *86*(1–2), 50–76. https://doi.org/10.1016/j.lithos.2005.04.003

D'Orazio, M., Agostini, S., Innocenti, F., Haller, M. J., Manetti, P., & Mazzarini, F. (2001). Slab windowrelated magmatism from southernmost South America: The late Miocene mafic volcanics from the Estancia Glencross area (~52 S, Argentina– Chile). *Lithos*, *57*(2–3), 67–89. https://doi.org/10.1016/s0024-4937(01)00040-8

Jackson, S. E., Pearson, N. J., Griffin, W. L., & Belousova, E. A. (2004). The application of laser ablation–inductively coupled plasma–mass spectrometry to in situ U–Pb zircon geochronology. *Chemical Geology*, *211*(1–2), 47–69. https://doi.org/10.1016/j.chemgeo.2004.06.017

Ludwig, K. R. (2003). *User's manual for Isoplot 3.0. A geochronological toolkit for Microsoft Excel*. Berkeley Geochronology Center Special Publication No.4.

McKenzie, D., & O'Nions, R. K. (1991). Partial melt distribution from inversion of rare earth element concentrations. *Journal of Petrology*, *32*(5), 1021–1091. https://doi.org/10.1093/petrology/32.5.1021

Paton, C., Woodhead, J. D., Hellstrom, J. C., Hergt, J. M., Greig, A., & Maas, R. (2010). Improved laser ablation U-Pb zircon geochronology through robust downhole fractionation correction. *Geochemistry, Geophysics, Geosystems*, *11*(3), Q0AA06. https://doi.org/10.1029/2009gc002618

Sláma, J., Kosler, J., Condon, D. J., Crowley, J. L., Gerdes, A., Hanchar, J. M., et al. (2008). Plesovice zircon – A new natural reference material for U–Pb and Hf isotopic microanalysis. *Chemical Geology*, *249*(1–2), 1–35. https://doi.org/10.1016/j.chemgeo.2007.11.005

Sun, S. S., & McDonough, W. F. (1989). Chemical and isotopic systematics of oceanic basalts; implications for mantle composition and processes. In A. D. Saunders & M. J. Norry (Eds.), *Magmatism in the ocean basins*, *Geological Society Special Publications* (Vol. 42(1), pp. 313–345). https://doi.org/10.1144/gsl.sp.1989.042.01.19

Whalen, J. B., Currie, K. L., & Chappell, B. W. (1987). A-type granites: Geochemical characteristics, discrimination and petrogenesis. *Contributions to Mineralogy and Petrology*, *95*(4), 407–419. https://doi.org/10.1007/bf00402202

Yang, Y., Zhang, H., Chu, Z., Xie, L., & Wu, F. (2010). Combined chemical separation of Lu, Hf, Rb, Sr, Sm and Nd from a single rock digest and precise and accurate isotope determinations of Lu–Hf, Rb–Sr and Sm–Nd isotope systems using Multi–Collector ICP–MS and TIMS. *International Journal of Mass Spectrometry*, *290*(2–3), 120–126. https://doi.org/10.1016/j.ijms.2009.12.011

19448007, 2024, 10, Downloaded from https://agupubs.onlinelibrary.wiley.com/doi/10.1029/2024GL109028 by Naturhistoriska Riksmuseet, Wiley Online Library on [15/12/2024]. See the Terms and Conditions (https://onlinelibrary.wiley.com/terms-and-conditions) on Wiley Online Library for rules of use; OA articles are governed by the applicable Creative Commons License